1

Calibration of a Structured Light System Using Planar Objects

Koichiro Yamauchi, Hideo Saito and Yukio Sato
Keio University
Japan

1. Introduction

A triangulation-based structured light system consists of a camera and a projector. The system is similar to passive stereo vision system whose camera is replaced by the projector. Various light projection techniques, e.g. light section method and space encoding method, have been proposed (Shirai, 1972; Posdamer & Altschuler, 1982). These methods allow us to recover the 3D shape by the camera observing a light stripe projected from the projector. Then, the system using an electrically controlled liquid crystal device (Sato & Inokuchi, 1987) and the system using a semiconductor laser and a synchronized scanned mirror (Sato & Otsuki, 1993) have been proposed. These systems capture accurate 3D shape at high speed using highly intense light stripes.

Typically, the geometry of a structured light system is expressed by the pinhole model (Bolles et al., 1981). The camera geometry is represented by a 3 x 4 matrix having 11 degrees of freedom and the projector geometry is represented by a 2 x 4 matrix having 7 degrees of freedom. The two matrices allow 3D reconstruction of a target object (Li et al., 2003; Fukuda et al., 2006; Zhang et al., 2007). Although the pinhole model is suited for the camera geometry, it is not applicable to the projector geometry. For example, light stripes do not always pass through the optical center of the projector using a rotatable mirror, e.g. galvanometer mirror and polygon mirror.

Subsequently, the triangulation principle based on the baseline is also utilized for a structured light system. Given one side and two angles of a triangle determine the position of a target object. One side is the baseline which is defined as the distance between the camera and the projector. One of the angles indicates camera view and the other angle indicates projector view. The invariable baseline model (Matsuki & Ueda, 1989; Sansoni et al., 2000) fails to represent some projectors using a rotatable mirror, but the variable baseline model (Hattori & Sato, 1996; Reid, 1996) eases this problem. However, these models assume that a light stripe is vertical to the baseline. It is preferable to express the light stripe by a 3D plane disregarding the inner structure of the projector.

In this chapter, we present a new geometric model and calibration method for a structured light system to overcome the problems. The geometric model is defined such that the camera model is based on the pinhole model and the projector model is based on the equation of a plane model. If light stripes are projected in different directions, their

projections are expressed accurately. In addition, the coefficients of the equation of a plane are estimated by observing a planar object from three viewpoints. It facilitates the procedure of user's tasks and provides a high degree of accuracy. Experimental results and comparisons demonstrate the effectiveness of our approach.

2. Geometric Model

A structured light system consists of a camera and a projector. The system captures a range data by the camera observing a target object illuminated from the projector. Fig. 1 is the geometric model of a structured light system. The camera model is based on the pinhole model and the projector model is based on the equation of a plane model. The geometric model is represented in the camera coordinate system and the reference plane is represented in the reference plane coordinate system.

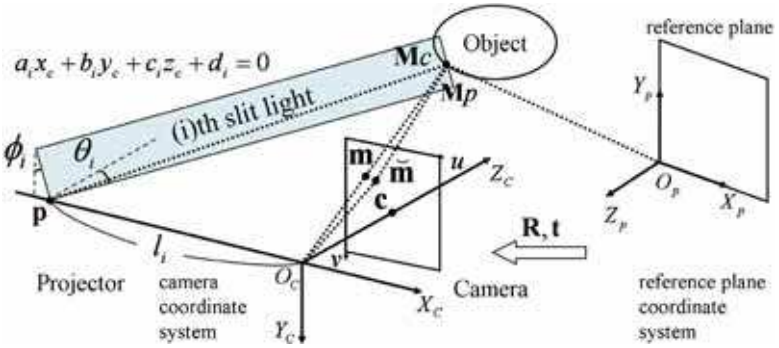

Fig. 1. Geometric model of a structured light system.

2.1 Camera model

Pinhole model is defined that light rays from an object pass through the optical center O_c for imaging. The principal point $\mathbf{c}$ at the intersection of the optical axis with the image plane is denoted by $[u_0, \quad v_0]$. X_c axis, Y_c axis, and Z_c axis are parallel to horizontal axis, vertical axis, and optical axis of the image plane. Here, a 2D point, i.e. image coordinates, $\mathbf{m}$ is denoted by $[u, \quad v]$ in the image plane, and a 3D point, camera coordinates, $\mathbf{M}_c$ is denoted by $[x_c, \quad y_c, \quad z_c]$ in the camera coordinate system $(O_c - X_c - Y_c - Z_c)$. In addition, X_p axis, Y_p axis, Z_p axis, and O_p are defined as horizontal axis, vertical axis, orthogonal axis, and the coordinate origin of the reference plane. Here, a 3D point, i.e. reference plane coordinates, $\mathbf{M}_p$ is denoted by $[x_p, \quad y_p, \quad z_p]$ in the reference plane coordinate system $(O_p - X_p - Y_p - Z_p)$. The perspective projection which maps the reference plane coordinates onto the image coordinates is given by

$$\tilde{\mathbf{m}} \cong \mathbf{A}\begin{bmatrix}\mathbf{R} & \mathbf{t}\end{bmatrix}\tilde{\mathbf{M}}_p \quad \text{with} \quad \mathbf{A} = \begin{bmatrix}\alpha & \gamma & u_0 \\ 0 & \beta & v_0 \\ 0 & 0 & 1\end{bmatrix} \tag{1}$$

where $\mathbf{A}$ is the camera intrinsic matrix with the scale factors, α, β, γ, and the principal point, u_0, v_0, i.e. the intrinsic parameters, and $[\mathbf{R} \quad \mathbf{t}]$ combines the rotation matrix and the translation vector, i.e. the extrinsic parameters. The tilde indicates the homogeneous coordinate by adding 1 for the additional element: $\tilde{\mathbf{m}} = [u, \quad v, \quad 1]$ and $\tilde{\mathbf{M}}_p = [x_p, \quad y_p, \quad z_p, \quad 1]$. The Euclidean transformation which transforms the reference plane coordinates to the camera coordinates is given by

$$\mathbf{M}_c \cong \begin{bmatrix}\mathbf{R} & \mathbf{t}\end{bmatrix}\tilde{\mathbf{M}}_p \quad \text{with} \quad \mathbf{R} = \begin{bmatrix}\mathbf{r}_1 & \mathbf{r}_2 & \mathbf{r}_3\end{bmatrix} \tag{2}$$

where $\mathbf{r}_1$, $\mathbf{r}_2$, $\mathbf{r}_3$ correspond to unit vectors to indicate the directions of X_p axis, Y_p axis, Z_p axis, respectively. $\mathbf{t}$ is the direction vector from O_p to O_c. Therefore, camera parameters provide the perspective projection and the Euclidian transformation. For more detail on camera geometry, refer to computer vision literatures (Faugeras & Luong, 2001; Hartley & Zisserman, 2004).

Let us consider camera lens distortion and its removal. The radial distortion causes the inward or outward displacement of the image coordinates from their ideal locations. This type of distortion is mainly caused by flawed radial curvature curve of the lens elements (Weng et al., 1992). Here, a distorted 2D point, i.e. real image coordinates, $\breve{\mathbf{m}}$ is denoted by $[\breve{u}, \quad \breve{v}]$. The discrepancy between the ideal image coordinates and the real image coordinates considering first two terms of radial distortion is given by

$$\breve{u} = u + (u - u_0)\left[k_1(x^2 + y^2) + k_2(x^2 + y^2)\right]^2 \tag{3}$$

$$\breve{v} = v + (v - v_0)\left[k_1(x^2 + y^2) + k_2(x^2 + y^2)\right]^2 \tag{4}$$

where k_1 and k_2 are the coefficients of the radial distortion, the center of which is the principal point. The normalized image coordinates $[x, \quad y]$ which suppose that the focal length is 1 (Wei & Ma, 1994) is give by

$$\begin{bmatrix}x \\ y \\ 1\end{bmatrix} = \mathbf{A}^{-1}\begin{bmatrix}u \\ v \\ 1\end{bmatrix} \tag{5}$$

Therefore, camera lens distortion can be corrected from captured images.

2.2 Projector model

The projector emits one to hundreds of light stripes for the measurement. We consider the case in which the light stripes are projected in different directions. It is difficult to assume that the projector model is based on the pinhole model, because they do not pass through the optical center. Therefore, we use the equation of a plane model to accurately represent the projector considering the projection of the light stripes which depend on the type of projector. In the camera coordinate system, the light stripe can be written as

$$a_i x_c + b_i y_c + c_i z_c + d_i = 0 \tag{6}$$

where i is the light stripe number, and a_i, b_i, c_i, d_i are the coefficients of the equation. There are an equal number of the equations of planes and the light stripes.

We define l_i is the baseline, i.e. the distance between the optical center of the camera and the light stripe of the projector, θ_i is the projection angle, i.e. the angle between Z_c axis and the light stripe, and ϕ_i is the tilt angle, i.e. the angle between Y_c axis and the light stripe. From the coefficients of the equation, these explicit parameters can be written as

$$l_i = d_i / a_i \tag{7}$$

$$\theta_i = \arctan(-c_i / a_i) \tag{8}$$

$$\phi_i = \arctan(-b_i / a_i) \tag{9}$$

Projector parameters are expressed by both implicit and explicit representations. The coefficients are used for computation of range data, but their values do not exhibit distinct features. In contrast, the baselines, projection angles, and tilt angles provide characteristic distributions.

2.3 Triangulation

To achieve range data, the projector emits light stripes to a target object, and then the camera observes the illuminated object. So, the camera coordinates is the intersection of the viewpoint of the camera and the equation of a plane of the projector. The linear equation $\left[x_c / z_c, \quad y_c / z_c, \quad 1\right]$ which is derived from (1), (2), and (6) is given by

$$\begin{bmatrix} \alpha & \gamma & 0 \\ 0 & \beta & 0 \\ a_i & b_i & d_i \end{bmatrix} \begin{bmatrix} x_c / z_c \\ y_c / z_c \\ 1 / z_c \end{bmatrix} = \begin{bmatrix} u - u_0 \\ v - v_0 \\ -c_i \end{bmatrix} \tag{10}$$

Consequently, we have

$$x_c = \frac{(u - u_0) - \gamma / \beta (v - v_0)}{\alpha} z_c \tag{11}$$

$$y_c = \frac{v - v_0}{\beta} z_c \tag{12}$$

$$z_c = \frac{d_i / a_i}{-c_i / a_i - \frac{(u-u_0) - \gamma/\beta(v-v_0)}{\alpha} - b_i / a_i \frac{(v-v_0)}{\beta}} \tag{13}$$

The coordinate z_c is computed by the relationship between the viewpoint of the camera and the equation of a plane of the projector. Then, the coordinate x_c and the coordinate y_c are computed by the similar triangle related to the camera. Therefore, the camera coordinates can be recovered by the camera and projector parameters.

The coordinate z_c which is expressed by the baseline, projection angle, and tilt angle instead of the coefficients can be written as

$$z_c = \frac{l_i}{\tan\theta_i - \frac{(u-u_0) - \gamma/\beta(v-v_0)}{\alpha} - \tan\phi_i \frac{(v-v_0)}{\beta}} \tag{14}$$

It indicates the triangulation principle based on one side and two angles of a triangle.

3. Calibration Method

In this section, we present a calibration method for a structured light system by observing a planar object from three viewpoints. Fig.2 is the calibration scene of a structure light system. The planar object, called reference plane, contains a checkered pattern, so that calibration points are detected as the intersection of line segments. To perform the calibration, the reference plane coordinates is assigned to the calibration points. Three sets of color images and slit light images, which include calibration points and light stripes on the reference planes respectively, are required. Our approach incorporates two separate stages: camera calibration and projector calibration.

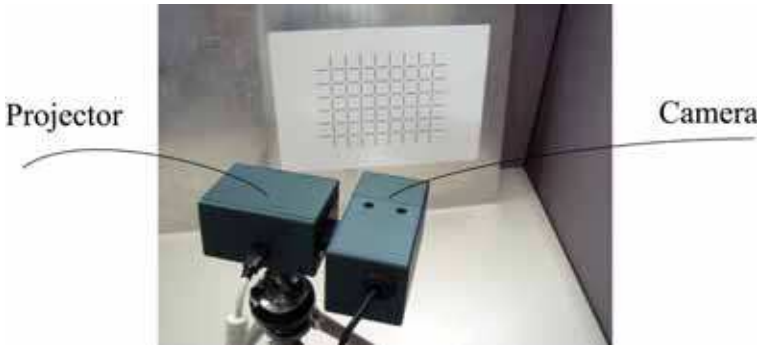

Fig. 2. Calibration scene.

3.1 Camera calibration

In the camera calibration stage, camera parameters are obtained by Zhang's method (Zhang, 2000). Fig. 3 shows the relationship between the reference plane and the image plane. The camera parameters are estimated by the correspondence between the reference plane coordinates and the image coordinates. Here, three color images must be captured from different positions changing orientations. If the reference plane undergoes pure translation, the camera parameters cannot be estimated (Zhang, 1998).

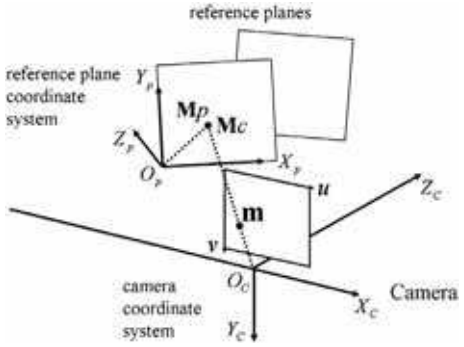

Fig. 3. Camera calibration.

3.2 Projector calibration

In the projector calibration stage, projector parameters are estimated by image-to-camera transformation matrix based on the perspective projection and the Euclidian transformation of the camera parameters which encapsulate the position and orientation of the reference planes. Fig. 4 shows the relationship among the reference plane, the image plane, and the light stripe. Here, the reference plane is on $z_p = 0$ and the coupled matrix $\mathbf{Q}$ is denoted by $[\mathbf{r}_1 \quad \mathbf{r}_2 \quad \mathbf{t}]$. From (1), the perspective projection which maps the reference plane coordinates onto the image coordinates can be written as

$$\tilde{\mathbf{m}} \cong \mathbf{A}\mathbf{Q}\begin{bmatrix} x_p \\ y_p \\ 1 \end{bmatrix} \tag{15}$$

From (2), the Euclidean transformation which transforms the reference plane coordinates to the camera coordinates can be written as

$$\mathbf{M}_c = \mathbf{Q}\begin{bmatrix} x_p \\ y_p \\ 1 \end{bmatrix} \tag{16}$$

Furthermore, the inverse of the coupled matix is given by

$$\mathbf{Q}^{-1} = \frac{1}{\mathbf{r}_3{}^{\mathrm{T}}\mathbf{t}} \begin{bmatrix} (\mathbf{r}_2 \times \mathbf{t})^{\mathrm{T}} \\ (\mathbf{t} \times \mathbf{r}_1)^{\mathrm{T}} \\ \mathbf{r}_3{}^{\mathrm{T}} \end{bmatrix} \tag{17}$$

where T indicates the transpose of a matrix. From (15), (16), and (17), the transformation matrix which maps the image coordinates into the camera coordinates is given by

$$\begin{aligned} \widetilde{\mathbf{M}}_c &= \begin{bmatrix} \mathbf{M}_c \\ 1 \end{bmatrix} = \begin{bmatrix} \mathbf{Q}^{\mathrm{T}} \\ \mathbf{k} \end{bmatrix} \begin{bmatrix} x_p \\ y_p \\ 1 \end{bmatrix} \\ &\cong \begin{bmatrix} \mathbf{Q}^{\mathrm{T}} \\ \mathbf{k} \end{bmatrix} \mathbf{Q}^{-1}\mathbf{A}^{-1}\widetilde{\mathbf{m}} \\ &\cong \begin{bmatrix} \mathbf{I} \\ (\mathbf{r}_3{}^{\mathrm{T}}\mathbf{t})^{-1}\mathbf{r}_3{}^{\mathrm{T}} \end{bmatrix} \mathbf{A}^{-1}\widetilde{\mathbf{m}} \end{aligned} \tag{18}$$

where the matrix $\mathbf{I}$ is denoted by $diag(1,1,1)$ and the vector $\mathbf{k}$ is denoted by $[0, \quad 0, \quad 1]$. The image-to-camera transformation matrix is directly estimated by camera parameters unlike other methods which necessitate recalculations. This matrix has eight degrees of freedom which is similar to the homography matrix in 2D.

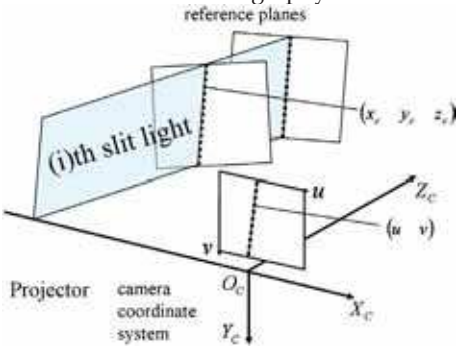

Fig. 4. Projector calibration.

For each light stripe, the image coordinates is transformed to the camera coordinates, so that the coefficients of the equation of a plane can be computed by the least square method at least three image coordinates. If the image coordinates of the light stripe are obtained from one reference plane, the equation of a plane cannot be computed. This is how all the light stripes are estimated.

3.3 Calibration procedure

The following is the recommended calibration procedure.

(a) Print a checkered pattern and attach it to a planar object
(b) Capture three sets of color images and slit light images from different position changing orientations by moving either the system or the plane
(c) Detect calibration points and correspond the image coordinates to the reference plane coordinates
(d) Estimate the camera parameters by Zhang's method
(e) Detect light stripes and correspond slit light numbers to the image coordinates
(f) Estimate the projector parameters by fitting a 3D plane as described in Sec. 3.2

4. Experimental Results

The data is captured by a structured light system, Cartesia 3D Handy Scanner of SPACEVISION. This system obtains range data in 0.5 seconds with 8 mm focal length, 640 x 480 pixels and 254 light stripes. The light stripes are scanned by a rotatable mirror (Hattori & Sato, 1996). The reference plane with the checkered pattern includes 48 calibration points with 20 mm horizontal and vertical intervals.

4.1 Calibration

Three sets of color images and slit light images are used for calibration as shown in Fig. 5. For the color images, one straight line is fitted to two horizontal line segments and the other straight line is fitted to two vertical segments. The calibration point is detected as the intersection of two straight lines. For slit light images, luminance values from 1 to 254 correspond to the light stripe number. The light stripes are projected to the reference plane vertically.

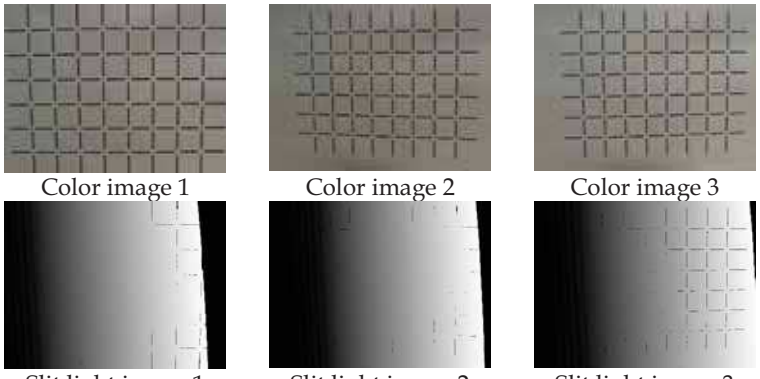

Color image 1 Color image 2 Color image 3

Slit light image 1 Slit light image 2 Slit light image 3

Fig. 5. Three sets of color images and slit light images.

Table 1 shows the camera intrinsic matrix and the coefficients of the radial distortion of the camera parameters. Fig. 6 shows the baselines, projection angles, and tilt angles of the projector parameters. When the light stripe number increases, the baselines gradually reduce, the projection angles increase, and the tilt angles remain almost constant. The camera and projector parameters enable the system to recover the camera coordinates of a target object.

A	$\begin{bmatrix} 1061.71 & -0.562002 & 350.08 \\ 0 & 1064.09 & 286.547 \\ 0 & 0 & 1 \end{bmatrix}$
k_1	-0.140279
k_2	-0.0916363

Table 1. Camera parameters.

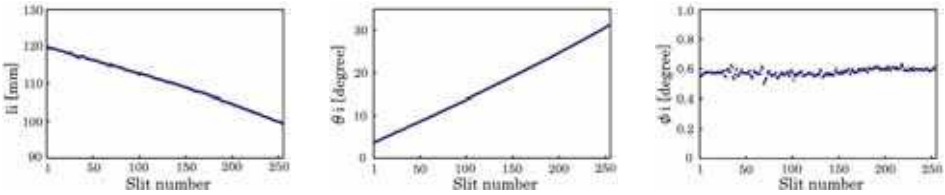

Baseline Projection angle Tilt angle

Fig. 6. Projector parameters.

4.2 Evaluation

We evaluated the measurement accuracy using five spheres with 25 mm radius placed in front of the system. In our evaluation, the system captures range data, and then fit the ideal spheres to them. The measurement accuracy which is defined as the distance between the ideal radius $\hat{r}$ and the real radius r_i is given by

$$E = \frac{1}{N}\sum_{i=1}^{N}(r_i - \hat{r})^2 \tag{19}$$

where N is the number of measuring points. To show the effectiveness, we evaluated our approach by comparing with two conventional approaches.

(i) The pinhole model calibrated by slide stage
The camera is modeled by the 3 x 4 projection matrix, and the projector is modeled by the 2 x 4 projection matrix. The camera and projector parameters are estimated using the slide stage.

(ii) The equation of a plane model calibrated by slide stage
The camera model is based on the pinhole model, and the projector model is based on the equation of a plane model. The camera parameters are obtained by Tsai's method (Tsai, 1987), and the projector parameters are estimated using the reference plane.

(iii) The equation of a plane model calibrated by reference plane: Our approach
The camera model is based on the pinhole model, and the projector model is based on the equation of a plane model. The camera and projector parameters are estimated using the reference plane.

Fig. 7 is the range data of five spheres. The spheres are numbered from top left to bottom right. In the approach (i), left two spheres, i.e. No. 1 and No. 4, and the ground are distorted in contrast to the approach (ii) and (iii). Table 2 shows the measurement accuracy of five spheres. In the approach (i), the measurement accuracy is higher than the approach (ii) and (iii). The approach (ii) and (iii) achieve similar performance. Therefore, the equation of a plane model is applicable to the structured light system. In addition, the reference plane as a planer object provides a high degree of accuracy and has a high degree of availability compared to the slide stage as a cubic object. The experimental results demonstrate the effectiveness and efficiency of our approach.


Approach (i)


Approach (ii)


Approach (iii)

Fig. 7. Range data of five spheres.

Sphere number	No. 1	No. 2	No. 3	No. 4	No. 5
Measuring points	15,629	15,629	19,405	19,861	19,861
Approach (i)	0.41	0.38	0.26	0.26	0.31
Approach (ii)	0.22	0.31	0.19	0.13	0.20
Approach (iii)	0.23	0.32	0.21	0.15	0.21

Table 2. Measurement accuracy of five spheres.

5. Future Work

It has been challenging to capture range data of an entire body using multiple projector-camera pairs. In our previous works, we have developed the system consisting of four pole units with sixteen projector-camera pairs (Yamauchi & Sato, 2006). Then, we have developed the system consisting of three pole units with twelve projector-camera pairs (Yamauchi et al., 2007). Fig. 8 is the human body measurement system. The system acquires range data in 2-3 seconds with 3 mm depth resolution and 2 mm measurement accuracy. The range data of a mannequin and a man are shown in Fig. 9 and Fig. 10, respectively. The numbers of measurement points are approximately 1/2 to one million. The projector-camera pairs are calibrated by our approach, and then their local coordinate systems are integrated into a single coordinate system by an automatic alignment approach (Fujiwara et al., 2008). Although Fujiwara's method is performed in two stages, our approach allows fully automatic calibration for this type of system. In addition, it is possible to facilitate the calibration process and reduce the implementation time.

Fig. 8. Human body measurement system.

6. Conclusions

We presented a novel geometric model and calibration method for a structured light system using a planar object. The geometric model is defined such that the camera model is based on the pinhole model and the projector is based on the equation of a plane model. Although the light stripes do not exactly pass through the optical center, our model can approximate the system geometry. In addition, the camera and projector parameters are estimated by observing a planar object from three viewpoints. The camera parameters are obtained by Zhang's method and the projector parameters are estimated by using image-to-camera transformation matrix. Furthermore, we verify our approach provides a high degree of accuracy in the experiments. In the future we intend to apply for the human body measurement system using multiple projector-camera pairs.

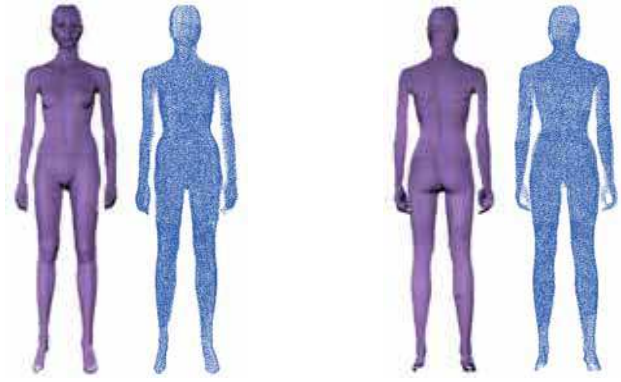

front back

Fig. 9. Range data of a mannequin.

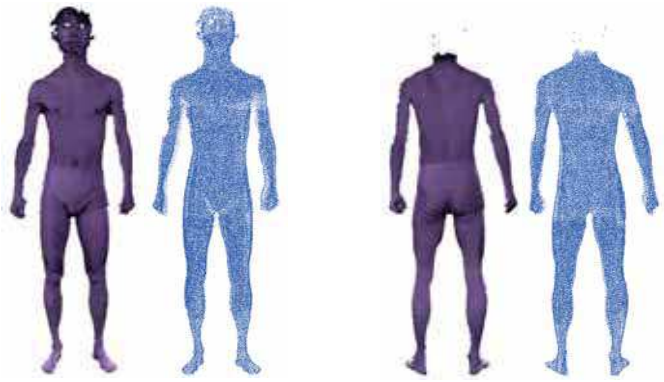

front back

Fig. 10. Range data of a man.

7. References

Bolles, R. C.; Kremers, J. H. & Cain, R. A. (1981). A simple sensor to gather three-dimensional data, *Technical Report 249,* (July 1981) Stanford Research Institute.

Faugeras, O. & Luong, Q. T. (2001). *The geometry of multiple images,* MIT Press, ISBN: 978-0262062206, Cambridge, MA, United States.

Fujiwara, K.; Yamauchi, K. & Sato, Y. (2008). An automatic alighnment technique for multiple rangefinders, *Proceedings of the SPIE,* Vol. 6805, (January 2008).

Fukuda, M.; Miyasaka, T. & Araki, K. (2006). A prototype system for 3D measurement using flexible calibration method, *Proceedings of the SPIE,* Vol. 6056, (January 2006).

Hartley, R. & Zisserman, A. (2004). *Multiple View Geometry in Computer Vision,* Cambridge University Press, ISBN: 978-0521540513, Cambridge, United Kingdom.

Hattori, K. & Sato, Y. (1996). Accurate rangefinder with laser pattern shifting, *Proceedings of the 13th International Conference on Pattern Recognition,* Vol. 3, (August 1996) pp. 849-853.

Li, Y. F. & Chen, S. Y. (2003). Automatic recalibration of an active structured light vision system, *IEEE Transactions on Robotics and Automation,* Vol. 19, No. 2, (April 2003) pp. 259-268.

Matsuki, M. & Ueda, T. (1989). A real-time sectional image measuring system using time sequentially coded grating method, *IEEE Transactions on Pattern Analysis and Machine Intelligence,* Vol. 11, No. 11, (Novemeber 1989) pp. 1225-1228.

Posdamer, J. L. & Altschuler, M. D. (1982). Surface measurement by space-encoded projected beam systems, *Computer Graphics and Image Processing,* Vol. 18, (January 1982) pp. 1-17.

Reid, I. D. (1996). Projective calibration of a laser-stripe range finder, *Image and Vision Computing,* Vol. 14, No. 9, (October 1996) pp. 659-666.

Sansoni, G.; Carocci, M. & Rodella, R. (2000). Calibration and performance evaluation of a 3-D imaging sensor based on the projection of structured light, *IEEE Transactions on Instrumentation and Measurement,* Vol. 49, No. 3, (June 2000) pp. 628-636.

Sato, K. & Inokuchi, S. (1987). Range-imaging system utilizing nematic liquid crystal mask, *Proceedings of the 1st International Conference on Computer Vision,* (June 1987) pp. 657-661.

Sato, Y. & Otsuki, M. (1993). Three-dimensional shape reconstruction by active rangefinder, *Proceedings of the 9th IEEE Conference on Computer Vision and Pattern Recognition,* (June 2003) pp. 142-147.

Shirai, Y. (1972). Recognition of polyhedrons with a range-finder, *Pattern Recognition*, Vol. 4, No. 3, (October 1972) pp. 243-250.

Tsai, R. Y. (1987). A versatile camera calibration technique for high-accuracy 3D machine vision metrology using off-the-shelf TV cameras and lens, *IEEE Journal of Robotics and Automation,* Vol. 3, No. 4, (August 1987) pp. 323-344.

Wei, G. & Ma, S. (1994). Implicit and explicit camera calibration: theory and experiments, *IEEE Transactions on Pattern Analysis and Machine Intelligence,* Vol. 16, No. 5, (May 1994) pp. 469-480.

Weng, J.; Cohen, P. & Herniou, M. (1992). Camera calibration with distortion models and accuracy evaluation, *IEEE Transactions on Pattern Analysis and Machine Intelligence,* Vol. 14, No. 10, (October 1992) pp. 965-980.

Yamauchi, K. & Sato, Y. (2006). 3D human body measurement by multiple range images, *Proceedings of the 18th International Conference on Pattern Recognition,* Vol. 4, (August 2006) pp. 833-836.

Yamauchi, K.; Kameshima, H.; Saito, H. & Sato, Y. (2007). 3D reconstruction of a human body from multiple viewpoints, *Proceedings of the 2nd Pacific-Rim Symposium on Image and Video Technology,* LNCS 4872, (December 2007) pp. 439-448.

Zhang, B.; Li, Y. F. & Wu, Y. H. (2007). Self-recalibration of a structured light system via plane-based homography, *Pattern Recognition,* Vol. 40, No. 4, (April 2007) pp. 1368-1377.

Zhang, Z. (1998). A flexible new technique for camera calibration, *Technical Report MSR-TR-98-71,* (December 1998) Microsoft Research.

Zhang, Z. (2000). A flexible new technique for camera calibration, *IEEE Transactions on Pattern Analysis and Machine Intelligence,* Vol. 22, No. 11, (November 2000) pp. 1330-1334.

Pattern Recognition
Edited by Peng-Yeng Yin

ISBN 978-953-307-014-8
Hard cover, 568 pages
Publisher InTech
Published online 01, October, 2009
Published in print edition October, 2009

For more than 40 years, pattern recognition approaches are continuingly improving and have been used in an increasing number of areas with great success. This book discloses recent advances and new ideas in approaches and applications for pattern recognition. The 30 chapters selected in this book cover the major topics in pattern recognition. These chapters propose state-of-the-art approaches and cutting-edge research results. I could not thank enough to the contributions of the authors. This book would not have been possible without their support.

INTECH
open science | open minds

InTech Europe
University Campus STeP Ri
Slavka Krautzeka 83/A
51000 Rijeka, Croatia
Phone: +385 (51) 770 447
Fax: +385 (51) 686 166
www.intechopen.com

InTech China
Unit 405, Office Block, Hotel Equatorial Shanghai
No.65, Yan An Road (West), Shanghai, 200040, China
中国上海市延安西路65号上海国际贵都大饭店办公楼405单元
Phone: +86-21-62489820
Fax: +86-21-62489821